Reductive amination of triglycerides to fatty amines over a titanium oxide-supported Pt–Mo catalyst

Katsumasa Sakoda,[a] Harumi Furugaki,[a] Sho Yamaguchi,[a,b,c] Takato Mitsudome [a,b,c]
and Tomoo Mizugaki *[a,b,d]

*Corresponding author: mizugaki.tomoo.es@osaka-u.ac.jp

[a] Department of Materials Engineering Science, Graduate School of Engineering Science, Osaka University, 1-3 Machikaneyama, Toyonaka, Osaka 560-8531, Japan

[b] Innovative Catalysis Science Division, Institute for Open and Transdisciplinary Research Initiatives (ICS-OTRI), Osaka University, Suita, Osaka 565-0871, Japan

[c] PRESTO, Japan Science and Technology Agency (JST), 4-1-8 Honcho, Kawaguchi, Saitama 333-0012, Japan

[d] Research Center for Solar Energy Chemistry, Graduate School of Engineering Science, Osaka University, 1-3 Machikaneyama, Toyonaka, Osaka 560-8531, Japan

Table of Content

1. General experimental details

Organic chemicals were purchased from Fujifilm Wako Pure Chemical Industries, Ltd., Tokyo Chemical Industry Co., Ltd., and Sigma-Aldrich, and were used as received. H_2PtCl_6, $RuCl_3$, K_3RhCl_6, and $Pd(NH_3)_4Cl_2$ hydrates were obtained from N. E. Chemcat. $(NH_4)_6Mo_7O_{24} \cdot 4H_2O$, NH_4VO_3, $(NH_4)_{10}(H_2W_{12}O_{42}) \cdot 4H_2O$, and $NaReO_4$ were purchased from Nacalai Tesque, Kishida Chemical, Sigma-Aldrich, and Alfa Aesar Co., Ltd., respectively. TiO_2 (SSP-N), ZrO_2 (RC-100), γ-Al_2O_3, and WO_3 were obtained from Sakai Chemical Industry Co., Ltd., Daiichi Kigenso Kagaku Kogyo Co., Ltd., Sumitomo Chemical Co., Ltd., and Fujifilm Wako Pure Chemical Industries, Ltd., respectively. Nb_2O_5 (JRC-NBO-2) was supplied by the Catalyst Society of Japan as the reference catalyst. Gas chromatography (GC-FID) analyses were performed on a Shimadzu GC-2030 instrument equipped with a capillary column (SH-Rtx-200MS, Shimadzu, 30 m × 0.25 mm i.d. film thickness 0.25 μm). Gas chromatography-mass spectrometry (GC-MS) analyses were performed on a Shimadzu QP-2010SE instrument equipped with a capillary column (SH-Rtx-200MS, Shimadzu, 30 m × 0.25 mm i.d. film thickness 0.25 μm, or InertCap WAX-HT, GL Science, 30 m × 0.25 mm i.d. film thickness 0.25 μm). ^1H and ^{13}C nuclear magnetic resonance (NMR) spectra were recorded using a JEOL JNM-ECS400 spectrometer. Chemical shifts are reported as follows: TMS (0 ppm for ^1H NMR) and $CDCl_3$ (77.1 ppm for ^{13}C NMR). NMR multiplicities are reported using the following abbreviations: s, singlet; d, doublet; t, triplet; q, quartet; m, multiplet; br, broad; J, coupling constants in hertz. Transmission electron microscopy (TEM) images were obtained using a Hitachi HF-2000 microscope instrument operating at 200 kV. High-angle annular dark-field scanning transmission electron microscopy (HAADF-STEM) images with elemental maps were collected using a JEOL JEM-ARM200F instrument, operated at 200 kV, and equipped with an energy-dispersive X-ray spectroscopy (EDX) detector. Pt L_3-edge and Mo K-edge X-ray absorption near-edge structure (XANES) spectra were recorded at room temperature in transmittance mode using Si (311) monochromators at the 01B1 beam line stations at SPring-8, Japan Atomic Energy Research Institute (JASRI), Harima, Japan (promotion number: 2024B1602). Data analysis was performed using Demeter ver. 0.9.21. X-ray photoelectron spectroscopy (XPS) spectra of the samples were obtained using a Shimadzu KRATOS ULTRA2 instrument, and the binding energy was referenced to the C 1s peak (285.0 eV). Inductively coupled plasma-atomic emission spectroscopy (ICP-AES) measurements was performed using a Perkin Elmer Optima 8300 instrument. Fourier-transform infrared (FT-IR) spectra were recorded using a JASCO FT-IR 4100 spectrometer equipped with a mercury cadmium telluride detector. The H_2 and NH_3-temperature programmed desorption (TPD) data were measured using a BELCAT-A instrument (BEL Japan Inc.) equipped with a thermal conductivity detector and mass spectrometer (BELMASSII, BEL Japan Inc.), respectively.

2. Catalyst preparation and reaction procedures

Preparation of metal oxide-supported Pt–Mo catalysts

The Pt–Mo/TiO$_2$ catalyst was prepared by co-impregnation method. Aqueous solution of H$_2$PtCl$_6$ (6.00 mL, 100 mM), (NH$_4$)$_6$Mo$_7$O$_{24}$·4H$_2$O (0.0265 g), and TiO$_2$ (1.000 g) were added to distilled water (50 mL) at room temperature. After stirring for 12 h in air, water was removed by rotary evaporation under reduced pressure to obtain the solid product. The obtained powder was dried at 110 °C for 5 h. After drying, the product was calcined at 500 °C for 3 h under a static air atmosphere to obtain Pt–Mo/TiO$_2$ as a gray powder. As determined using ICP-AES, the Pt and Mo contents in Pt–Mo/TiO$_2$ were 9.31 and 1.30 wt%, respectively. The other catalysts were prepared in a similar way using various metal salts and supports. All catalysts were applied to the reaction without any pre-reduction step.

Typical reductive amination procedure (Table 1, entry 1)

The reductive amination of trilaurin (**2**) with piperidine (**1**) was carried out in a 50 mL stainless steel autoclave equipped with a Teflon vessel. The vessel was charged with **1** (0.085 g, 1.0 mmol), **2** (0.320 g, 0.5 mmol), Pt–Mo/TiO$_2$ (0.150 g), and n-hexane (3.0 mL), and a Teflon-coated magnetic stir bar was added. The reactor was sealed, purged five times with 1.0 MPa H$_2$, and then pressurized (4.0 MPa), heated to 180 °C, and stirred at 900 rpm for 6 h. After the reaction, the autoclave was cooled in an ice-water bath, and H$_2$ gas was released. The resulting reaction mixture was diluted with ethanol and analyzed by GC-FID.

Product yields were calculated by the following equation:

$$\text{yield (based on } \mathbf{1}) = \frac{\text{amount of } \mathbf{3} \text{ (mmol)}}{\text{amount of loaded } \mathbf{1} \text{ (mmol)}} \times 100 \qquad \text{(eq. S1)}$$

$$\text{yield (based on } \mathbf{2}) = \frac{\text{amount of } \mathbf{3} \text{ (mmol)}}{\text{amount of loaded } \mathbf{2} \text{ (mmol)} \times 3} \times 100 \qquad \text{(eq. S2)}$$

In Table 2, entry 5, didodecylamine yield was calculated by the following equation:

$$\text{yield (based on } \mathbf{2}) = \frac{\text{amount of didodecylamine (mmol)} \times 2}{\text{amount of loaded } \mathbf{2} \text{ (mmol)} \times 3} \times 100 \qquad \text{(eq. S3)}$$

Catalyst reuse experiments (Fig. 1)

After the reductive amination was complete, the catalyst was separated from the reaction mixture by centrifugation, washed with ethanol and then with n-hexane in air before being reused in a subsequent reaction.

Gram-scale reaction (Scheme 2)

The gram-scale reductive amination was carried out in a 100 mL stainless steel autoclave equipped with a Teflon vessel. The vessel was charged with **1** (1.00 g, 11.7 mmol), **2** (3.50 g, 5.48 mmol), Pt–Mo/TiO$_2$ (1.00 g), and n-hexane (10.0 mL), and a Teflon-coated magnetic stir bar was added. The reactor was purged five times with 1.0 MPa H$_2$ and then pressurized to 4.0 MPa at room temperature, heated to 180 °C, and stirred at 900 rpm for 60 h. After the reaction, the autoclave was cooled in an ice-water bath, and the H$_2$ gas was carefully released. Pt–Mo/TiO$_2$ was separated by filtration, and n-hexane was evaporated. The residue was purified by silica gel chromatography with chloroform/methanol to give pure **3** (1.86 g, 7.36 mmol, 62%).

Pt–Mo/TiO$_2$ pre-reduction (Fig. 2b(iii), Table S7(iii), Table S9, and Scheme S1)

Pt–Mo/TiO$_2$ was pre-reduced for the experiments in Fig. 2b(iii), Table S7(iii), Table S9, and Scheme S1 under the typical reductive amination conditions without substrates: Pt–Mo/TiO$_2$ (0.150 g), n-hexane (3.0 mL), 180 °C, H$_2$ (4.0 MPa), 2 h.

Synthesis of 1-(1-piperidinyl)-1-dodecanone (4)

4 was prepared according to the literature procedure.[S1] The flask was charged with **1** (0.850 g, 10 mmol), lauroyl chloride (1.20 g, 5.5 mmol), and Et$_2$O (50.0 mL) in an ice-water bath, and a Teflon-coated magnetic stir bar was added. The solution was stirred at room temperature for 3 h. After the reaction, the solution was washed consecutively with aqueous HCl, aqueous NaOH, and brine. The organic phase was gathered, dried with anhydrous magnesium sulfate, evaporated, and dried under vacuum to give pure **4** (1.30 g, 4.84 mmol, 88%).

Analysis of the components of cooking oil (Table S6)

The cooking oil (Canola oil, J-OIL MILLS, Inc.) used in this study was analyzed according to the literature procedure.[S2] The flask was charged with cooking oil (0.040 g), n-hexane (1.0 mL), and KOH (1.0 mL, 0.4 M in methanol), and a Teflon-coated magnetic stir bar was added. The solution was sonicated for 2 h, and then stirred at room temperature for 12 h. After the reaction, water (2.0 mL) was added to the reaction mixture. The organic phase was analyzed by GC-MS using an internal standard method.

TPD-IR measurements (Fig. S8)

A thin disk of the sample was prepared by pressing the sample powder onto a stainless steel grid. The sample disk was then placed inside an IR cell to enable thermal treatment in a controlled atmosphere. The sample pellet was treated under vacuum at 180 °C for 1 h before the introduction of probe molecules. The sample was pretreated under 1 bar of H_2 at 180 °C for 1 h and then outgassed. Then, the sample was cooled to 50 °C, and treated with vaporized acetone (27 mbar) at 50 °C for 5 min. FT-IR spectra were recorded after the desorption of physisorbed or weakly chemisorbed species under vacuum at 50 °C. After the IR spectrum at 50 °C was taken, the sample was heated to a desired temperature under vacuum, and the spectrum was measured after keeping at the same temperature for 10 min.

3. Supplementary tables

As shown in Table S1, in *n*-hexane solvent, 54% conversion of **1** and 35 % yield of **3** was obtained, while tetrahydrofuran was an ineffective solvent for the reductive amination. We think that the oxygen-containing solvents, such as tetrahydrofuran, may strongly adsorb on the catalyst active sites, thus suppressing the interaction of substrates with the active sites. Nonpolar *n*-hexane will not adsorb on the surface, allowing the facile adsorption of the substrates on the active sites. Ethanol solvent reacted with **1** to produce 1-ethylpiperidine. This result is consistent with the result of the control experiment using **1** and 1-dodecanol (**7**) in Fig. 2b(ii-2).
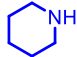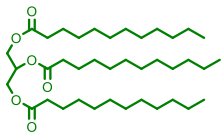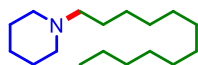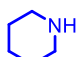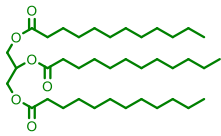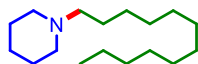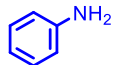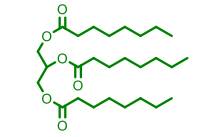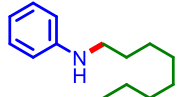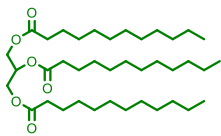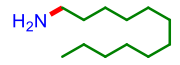
Table S1 Reductive amination of **1** with **2** using Pt–Mo/TiO$_2$ in various solvents
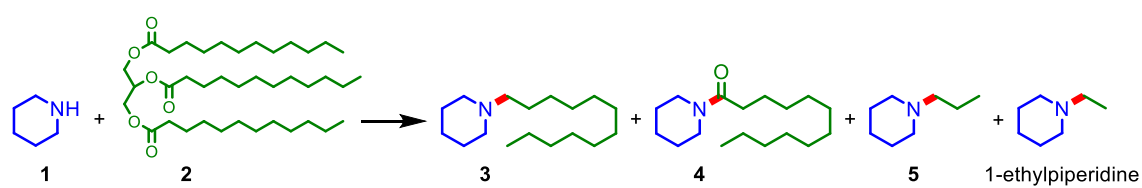
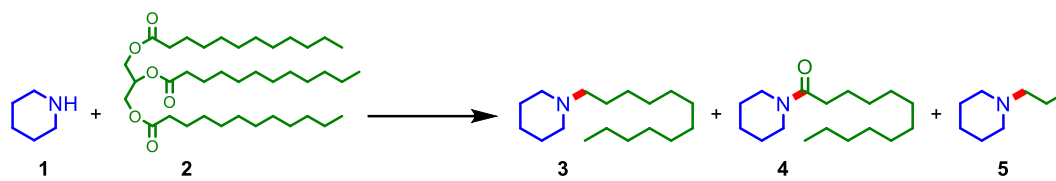| entry	solvent	conv. of **1** (%)	yield based on **1** (%)			
			3	**4**	**5**	1-ethylpiperidine
1	*n*-hexane	54	35	4	3	-
2	tetrahydrofuran	31	3	4	0	-
3	ethanol	>99	0	0	0	>99

Reaction conditions: catalyst (0.15 g, Pt: 7 mol% and Mo: 2 mol%), **1** (1 mmol), **2** (0.5 mmol), solvent (3 mL), 180 °C, H$_2$ (4 MPa), 6 h.

Table S2 Comparison of activity between Pt–Mo/TiO$_2$ and previously reported catalysts in the reductive amination of triglycerides under H$_2$

catalyst	amine	triglyceride	product	reaction conditions	ref.
Pt–Mo/TiO$_2$			70% yield	n-hexane, 4 MPa H$_2$, 180 °C, 16 h	**this work** Table 1, entry 2
Pt–Mo/TiO$_2$			61% yield	n-hexane, 1 MPa H$_2$, 180 °C, 60 h	**this work** Table 1, entry 3
Ru(acac)$_3$ (1,1,1-tris(diphenylphosphinomethyl)ethane (triphos) Trifluoromethanesulfonimide (HNTf$_2$)			89% yield	tetrahydrofuran 6 MPa H$_2$, 130 °C, 18 h	S3
ZnO$_2$–Al$_2$O$_3$	NH$_3$	coconuts oil		25 MPa H$_2$, 310 °C	S4
Pt/ZrO$_2$	NH$_3$		59% yield	water, 5.5 MPa H$_2$, 220 °C, 36 h	S5

We performed reuse experiments using Pt–Mo/TiO$_2$ and Pt–Mo/γ-Al$_2$O$_3$ with similar catalytic activities (Table S3). Pt–Mo/TiO$_2$ could be reused 10 times without loss of its activity (Fig. 1). In contrast, the conversion with Pt–Mo/γ-Al$_2$O$_3$ decreased from 99% to 89%, maybe due to the decrease of the acid amounts. Therefore, Pt–Mo/TiO$_2$ was selected as the most suitable catalyst in terms of activity and durability.
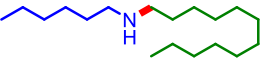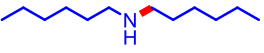
Table S3 Reusability of Pt–Mo catalysts
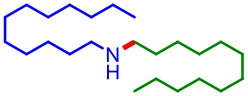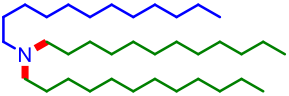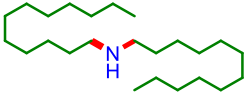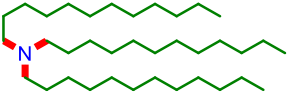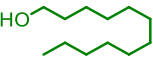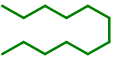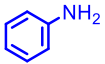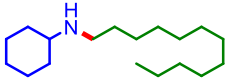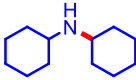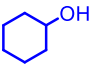
entry	catalyst	conv. of **1** (%)	yield based on **1** (%)		
			3	**4**	**5**
1	fresh Pt–Mo/TiO$_2$	99	70	2	7
2	used Pt–Mo/TiO$_2$	>99	70	0	15
3	fresh Pt–Mo/γ-Al$_2$O$_3$	99	66	1	17
4	used Pt–Mo/γ-Al$_2$O$_3$	89	53	2	10

Reaction conditions: catalyst (0.15 g, Pt: 7 mol% and Mo: 2 mol%), **1** (1 mmol), **2** (0.5 mmol), *n*-hexane (3 mL), 180 °C, H$_2$ (4 MPa), 16 h.

Table S4 ICP-AES analyses of fresh and used Pt–Mo/TiO$_2$

sample	amount (wt%)			atomic ratio		
	Pt	Mo	Ti	Pt/Ti	Mo/Ti	Mo/Pt
fresh Pt–Mo/TiO$_2$	9.31	1.30	46.2	0.0494	0.0140	0.284
used Pt–Mo/TiO$_2$	9.16	1.26	45.8	0.0491	0.0137	0.280

Table S5 Detailed product analysis of the substrate scope in the reductive amination of **2**

amine	time (h)	conv. of amine (%)	product and yield based on amine (%)			
(pentylamine, NH₂)	36	>99	35	11	1	
(dodecylamine, NH₂)	36	>99	70	26		
NH₃	36	-	74[a]	10[a]	4[a]	7[a]
(aniline, NH₂)	24	>99	46	32	2	

Reaction conditions: Pt–Mo/TiO₂ (0.15 g, Pt: 7 mol% and Mo: 2 mol%), amine (1 mmol), triglyceride (0.5 mmol), *n*-hexane (3 mL), 180 °C, H₂ (4 MPa). [a] Yield was based on **2**.

Table S6 The carboxylic acid contents of the cooking oil[a]

type of carboxylic acid	C16	C18:0	C18:1	C18:2
content (mmol/g)	0.17	0.07	2.67	0.62

[a] For C18:X, X is the number of C=C bonds in carboxylic acids

**Table S7** Detailed product analysis of control experiments in Fig. 2b

	substrate	time (h)	catalyst	conv. of 1 (%)	yield (%)			
					3[a]	4[a]	7[b]	8[b]
i	2 (0.5 mmol)	2	Pt–Mo/TiO$_2$	-	-	-	15	63
			Pt/TiO$_2$	-	-	-	7	21
ii-1	1 (1 mmol) 6 (1.5 mmol)	0.5	Pt–Mo/TiO$_2$	>99	85	-	23	6
			Pt/TiO$_2$	>99	86	-	23	<1
ii-2	1 (1 mmol) 7 (1.5 mmol)	2	Pt–Mo/TiO$_2$	37	25	-	-	19
			Pt/TiO$_2$	26	16	-	-	<1
iii[c]	1 (1 mmol) 2 (0.5 mmol)	4	Pt–Mo/TiO$_2$	58	-	24	-	-
			Pt/TiO$_2$	72	-	21	-	-
iv[d]	4 (1 mmol)	1	Pt–Mo/TiO$_2$	57	33	-	4	8
			Pt/TiO$_2$	23	10	-	7	<1

Reaction conditions: Pt–Mo/TiO$_2$ or Pt/TiO$_2$ (0.15 g; Pt: 4.8 mol% and Mo: 1.4 mol% with respect to the ester moiety for (i); Pt: 7 mol% and Mo: 2 mol% for (ii-1), (ii-2), (iii), (iv)), *n*-hexane (3 mL), 180 °C, H$_2$ (4MPa). [a] Yield was based on 1. [b] Yield was based on 2. [c] Catalyst was pre-reduced under 4 MPa H$_2$ at 180 °C for 2 h. The control experiment was conducted under Ar (0.1 MPa). [d] Conv. and yield were based on 4.

Table S8 The content of Mo species in used Pt–Mo/TiO$_2$ estimated by Mo 3d XPS spectrum

	binding energy (eV)	ratio (%)
Mo(0)	228.4	5.5
MoO$_2$	229.8	19.2
MoO$_y$	230.7	15.2
MoO$_z$	231.5	48.7
MoO$_3$	232.6	11.4

Table S9 Amidation of **2** with **1** under Ar using Pt–Mo catalysts
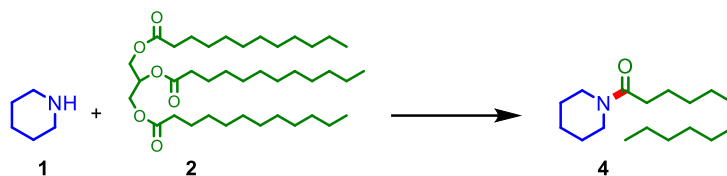
entry	catalyst	acid amount[b] (µmmol)	conv. of **1** (%)	yield of **4** based on **1** (%)
1	Pt–Mo/TiO$_2$	130	58	24
2	Pt–Mo/γ-Al$_2$O$_3$	132	50	21
3	Pt–Mo/Nb$_2$O$_5$	13	17	10

Reaction conditions: Pt–Mo catalyst (0.15 g; Pt: 7 mol% and Mo: 2 mol%), **1** (1 mmol), **2** (0.5 mmol), *n*-hexane (3 mL), 180 °C, Ar (0.1 MPa), 4 h. Catalyst was pre-reduced under 4 MPa H$_2$ at 180 °C for 2 h. [b] Measured by NH$_3$-TPD (Fig. S9).

4. Supplementary figures
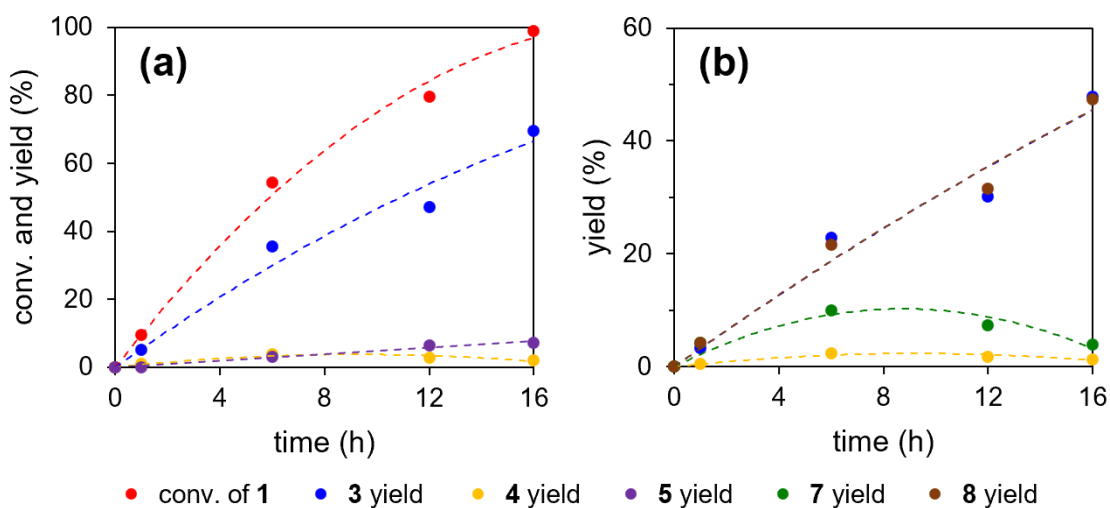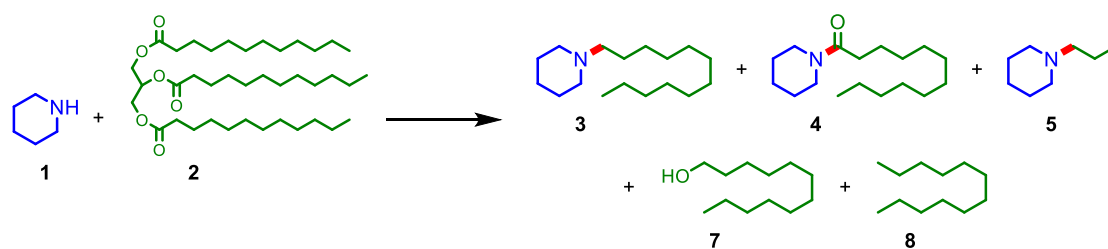
Fig. S1 Time-course data of the reductive amination of **2** with **1** catalyzed by Pt–Mo/TiO$_2$. Product yield was determined based on (a) **1** and (b) **2**. Reaction conditions: Pt–Mo/TiO$_2$ (0.15 g, Pt: 7 mol% and Mo: 2 mol%), **1** (1 mmol), **2** (0.5 mmol), *n*-hexane (3 mL), 180 °C, H$_2$ (4 MPa).
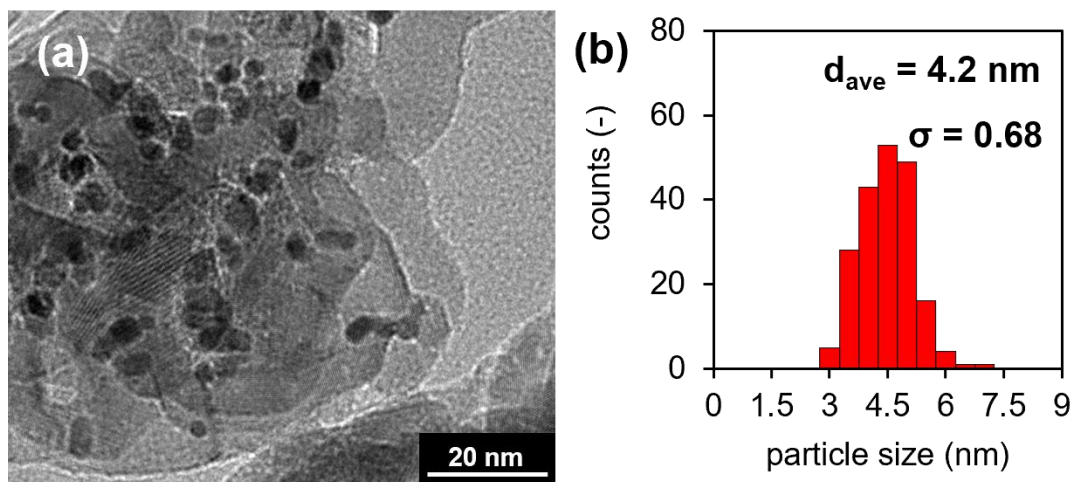
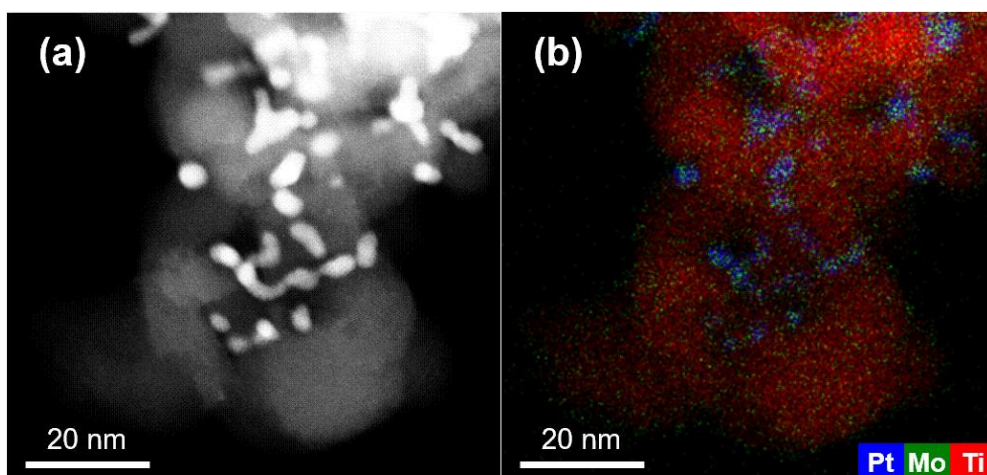**Fig. S2** (a) TEM image and (b) size distribution histogram of used Pt/TiO$_2$.

Fig. S3 (a) HAADF-STEM image of used Pt–Mo/TiO$_2$. (b) Composite overlay of the elemental mapping of Pt, Mo, and Ti in used Pt–Mo/TiO$_2$.
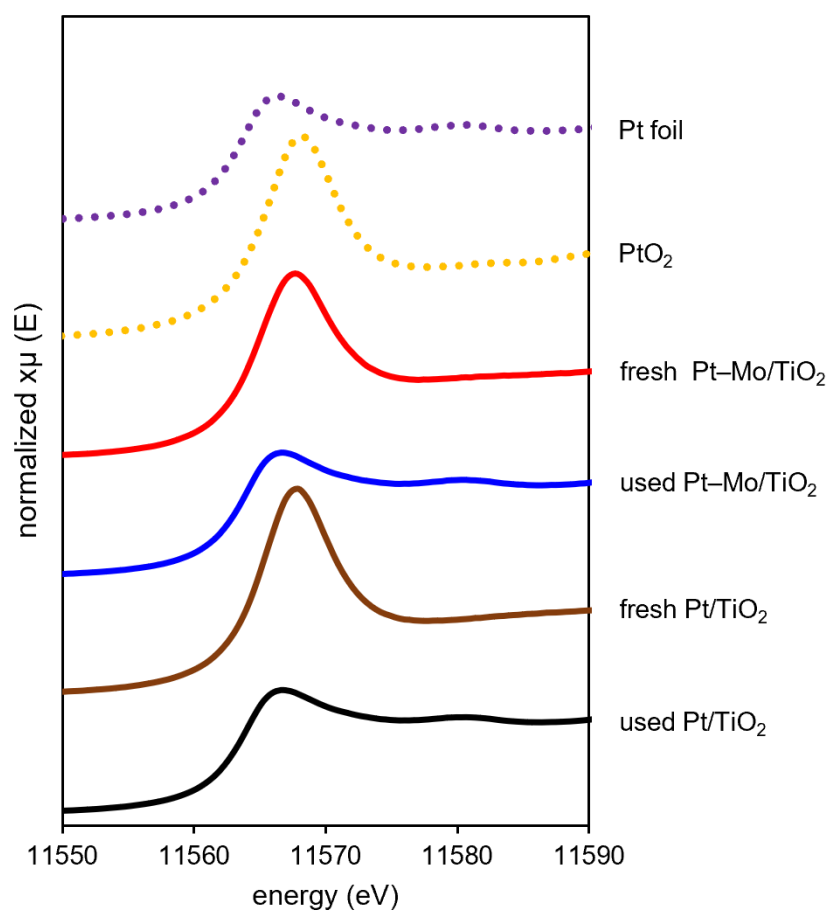
Fig. S4 Pt L_3-edge XANES spectra of Pt foil, PtO_2, fresh Pt–Mo/TiO_2, used Pt–Mo/TiO_2, fresh Pt/TiO_2, and used Pt/TiO_2.

Fig. S5 shows the Mo K-edge XANES spectra of the Pt–Mo/TiO$_2$ and Mo/TiO$_2$ catalysts. The absorption edge energy of the used Pt–Mo/TiO$_2$ was lower than that of fresh Pt–Mo/TiO$_2$, indicating the reduction of Mo species under the reductive amination conditions. In contrast, the absorption edge energies in the fresh and used Mo/TiO$_2$ were similar. These results confirm the H-spillover process, in which the hydrogen species on the Pt NPs are transported to reduce MoO$_3$.
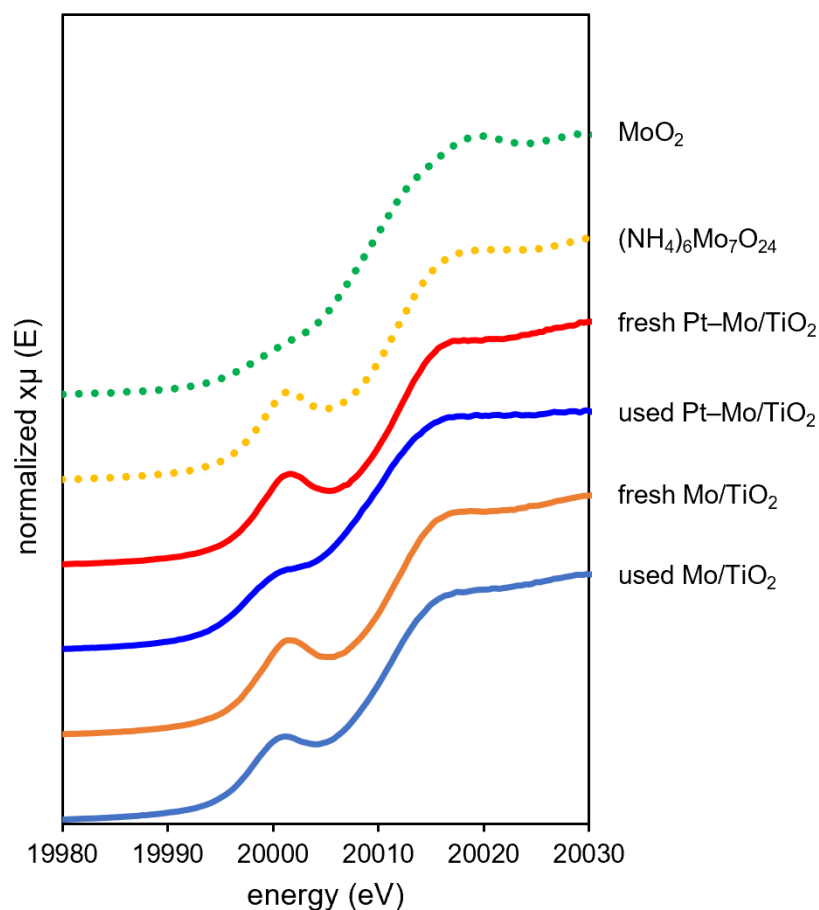
Fig. S5 Mo K-edge XANES spectra of MoO$_2$, (NH$_4$)$_6$Mo$_7$O$_{24}$, fresh Pt–Mo/TiO$_2$, used Pt–Mo/TiO$_2$, fresh Mo/TiO$_2$, and used Mo/TiO$_2$.

The XPS analysis of used Pt–Mo/TiO$_2$ and Pt/TiO$_2$ was also conducted to investigate the chemical state of the surface Pt species. The Pt 4f$_{7/2}$ peak of used Pt–Mo/TiO$_2$ and Pt/TiO$_2$ was observed at 70.6 eV and 70.4 eV, respectively (Fig. S6), which can be assigned to Pt(0). These XPS results are consistent with the Pt L$_3$-edge XANES analysis.
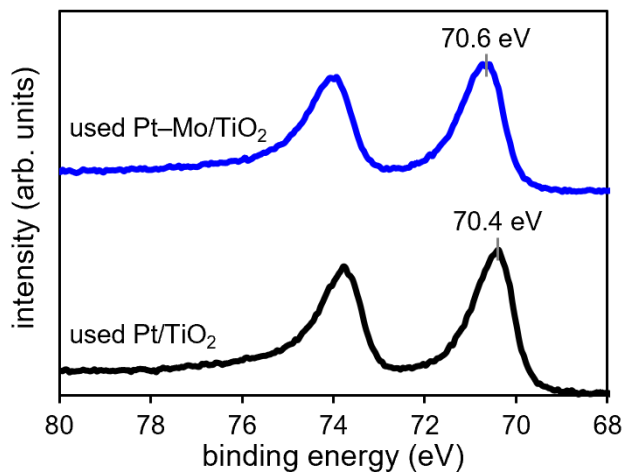
Fig. S6 XPS spectra in the Pt 4f region of used Pt–Mo/TiO$_2$ and Pt/TiO$_2$.

H_2-TPD measurements were performed using Pt–Mo/TiO$_2$ and Pt/TiO$_2$ to gain insight into the structure of MoO$_x$. Both H_2-TPD profiles display a broad peak at approximately 200 °C, and the corresponding H_2 desorption amounts were 101 and 133 µmol/g, respectively (Fig. S7). The lower amount of H_2 desorption for Pt–Mo/TiO$_2$ compared to that for Pt/TiO$_2$ would be due to the decrease of exposed Pt atoms and TiO$_2$ by covering with Mo species. The H_2-TPD profiles showed no obvious peaks assigned to H species on the Mo sites. Therefore, we could not obtain clear evidence of the presence of spillover hydrogen species adsorbed on the Mo species.
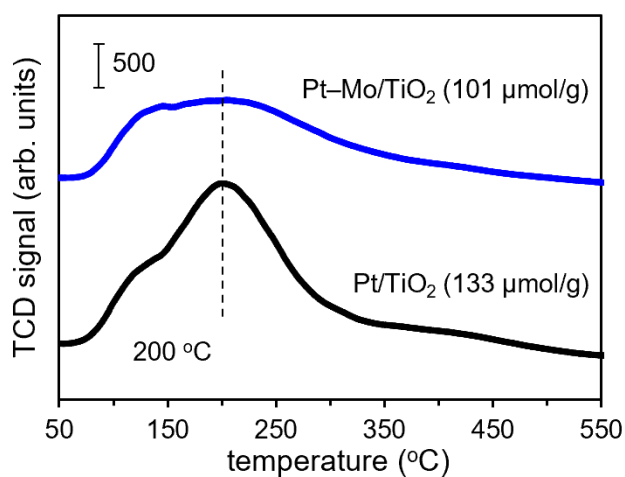
Fig. S7 H_2-TPD spectra of Pt–Mo/TiO$_2$ and Pt/TiO$_2$. H_2 desorption amounts are presented in parentheses.
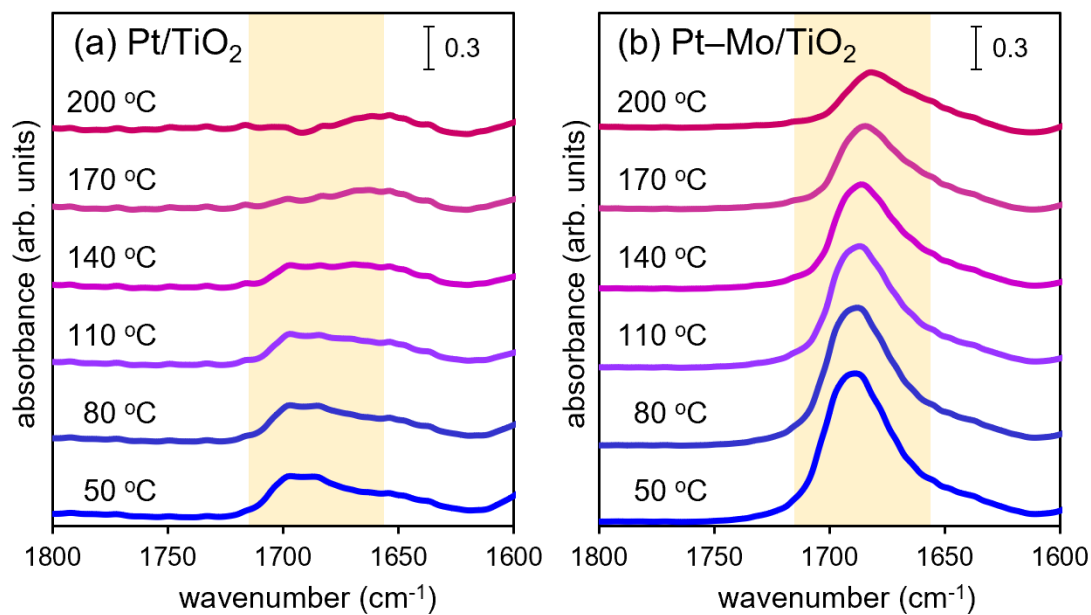
Fig. S8 TPD-IR spectra of acetone adsorbed on H_2-treated (a) Pt/TiO_2 and (b) $Pt–Mo/TiO_2$.
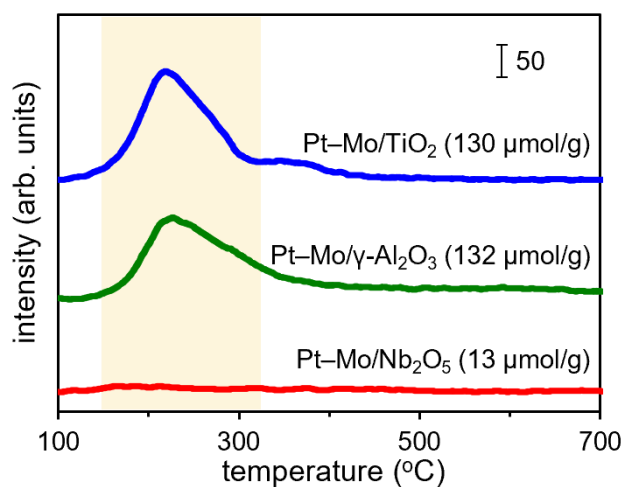
Fig. S9 NH_3-TPD profiles of $Pt–Mo/TiO_2$, $Pt–Mo/\gamma Al_2O_3$, and $Pt–Mo/Nb_2O_5$. Acid amounts at approximately 200 °C are presented in parentheses. NH_3 desorption was monitored by mass number m/z = 16 during heating.

5. Supplementary schemes

To investigate the influence of catalyst pre-reduction, Pt–Mo/TiO$_2$ was pre-reduced under 4 MPa H$_2$ at 180 °C for 2 h, and its activity was evaluated under the typical reaction conditions. The pre-reduced Pt–Mo/TiO$_2$ provided **3** in a 31% yield, which was comparable to that of unreduced Pt–Mo/TiO$_2$ (Scheme S1 vs Table 1, entry 1). This result indicates that the Pt and Mo species are rapidly reduced under the reaction conditions to form the active species.
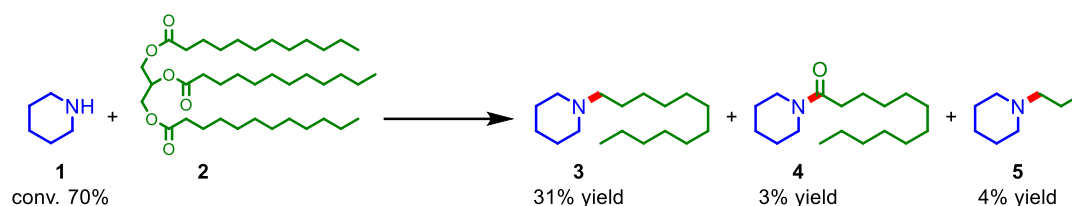
Scheme S1 Reductive amination of **2** with **1** using pre-reduced Pt–Mo/TiO$_2$. Reaction conditions: pre-reduced Pt–Mo/TiO$_2$ (0.15 g, Pt: 7 mol% and Mo: 2 mol%), **1** (1 mmol), **2** (0.5 mmol), *n*-hexane (3 mL), 180 °C, H$_2$ (4 MPa), 6 h.

To consider the formation of unidentified compounds, the thermal treatment of **1** was performed; **1** was stirred at 180 °C in the absence of Pt–Mo/TiO$_2$ and **2**, resulting in a 76% recovery of **1** (Scheme S2). This result indicates the thermal decomposition of **1** under the reaction conditions.[S6] However, it was not possible to identify based on MS analysis.
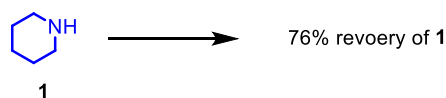
Scheme S2 Thermal decomposition of **1** under the reductive amination conditions. Reaction conditions: **1** (1 mmol), *n*-hexane (3 mL), 180 °C, H$_2$ (4 MPa), 6 h.

6. Product identification
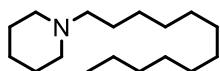
1-Dodecylpiperidine (3)

CAS registry No. [5917-47-5]. **^{1}H NMR** (400 MHz, CDCl$_3$): δ/ppm 2.37 (br-s, 4H), 2.31–2.23 (m, 2H), 1.64–1.55 (m, 4H), 1.55–1.38 (m, 4H), 1.38–1.20 (m, 18H), 0.88 (t, 3H, J = 7.0 Hz). **^{13}C NMR** (100 MHz, CDCl$_3$): δ/ppm 59.7, 54.7, 32.0, 29.74, 29.69, 29.4, 27.9, 27.0, 26.0, 24.6, 22.8, 14.2. **GC-MS** (EI): m/z 253 (M$^+$, 1%), 99 (8), 98 (100), 96 (1), 85 (1), 84 (2), 70 (2), 69 (2), 57 (1), 56 (1), 55 (5).
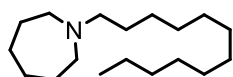

1-Dodecylazepane

CAS registry No. [20422-09-7]. **^{1}H NMR** (400 MHz, CDCl$_3$): δ/ppm 2.63 (t, 4H, J = 5.6 Hz), 2.49–2.42 (m, 2H), 1.69–1.55 (m, 8H), 1.52–1.41 (m, 2H), 1.35–1.19 (m, 18H), 0.88 (t, 3H, J = 6.8 Hz). **^{13}C NMR** (100 MHz, CDCl$_3$): δ/ppm 58.5, 55.6, 32.0, 29.74, 29.71, 29.4, 27.8, 27.7 27.5, 27.1, 22.8, 14.2. **GC-MS** (EI): m/z 267 (M$^+$, 1%), 113 (9), 112 (100), 110 (1), 98 (1), 84 (2), 70 (1), 69 (1), 58 (8), 57 (2), 56 (1), 55 (6).
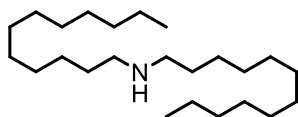
Didodecylamine

CAS registry No. [3007-31-6]. **^{1}H NMR** (400 MHz, CDCl$_3$): δ/ppm 2.58 (t, 4H, J = 7.2 Hz), 1.53–1.44 (m, 4H), 1.35–1.20 (m, 37H), 0.88 (t, 6H, J = 6.8 Hz). **^{13}C NMR** (100 MHz, CDCl$_3$): δ/ppm 50.3, 32.0, 30.3, 29.8, 29.71, 29.68, 29.4, 27.5, 22.8, 14.2. **GC-MS** (EI): m/z 353 (M$^+$, 2%), 352 (1), 254 (1), 212 (2), 200 (1), 199 (15), 198 (100), 196 (1), 186 (1), 185 (1), 184 (4), 112 (1), 98 (1), 86 (1), 85 (1),84 (2), 83 (1), 72 (1), 71 (2) 70 (4), 69 (4), 58 (1), 57 (9), 56 (4), 55 (8).
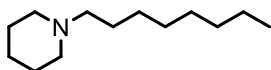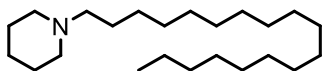
1-Octylpiperidine

CAS registry No. [7335-02-6]. **¹H NMR** (400 MHz, CDCl₃): δ/ppm **¹H NMR** (400 MHz, CDCl₃): δ/ppm 2.39 (br-s, 4H), 2.32–2.19 (m, 2H), 1.70–1.55 (m, 4H), 1.55–1.37 (m, 4H), 1.37–1.17 (m, 18H), 0.88 (t, 3H, J = 7.0 Hz). **¹³C NMR** (100 MHz, CDCl₃): δ/ppm 59.7, 54.7, 31.9, 29.6, 29.3, 27.8, 26.9, 25.9, 24.5, 22.7, 14.1. **GC-MS** (EI): m/z 197 (M⁺, 3%), 196 (1), 99 (7), 98 (100), 96 (1), 85 (1), 84 (2), 70 (4), 69 (2), 56 (2), 55 (5).
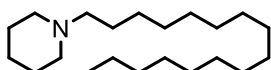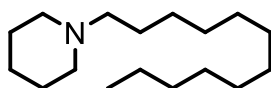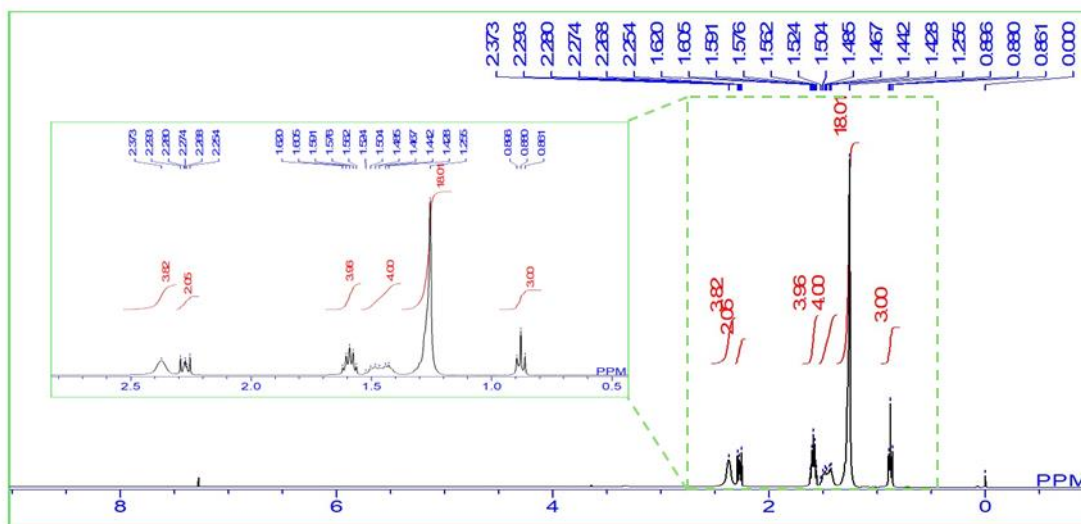

1-Hexadecylpiperidine

CAS registry No. [7335-03-7]. **¹H NMR** (400 MHz, CDCl₃): δ/ppm 2.36 (br-s, 4H), 2.30–2.22 (m, 2H), 1.64–1.55 (m, 4H), 1.54–1.38 (m, 4H), 1.38–1.18 (m, 26H), 0.88 (t, 3H, J = 6.8 Hz). **¹³C NMR** (100 MHz, CDCl₃): δ/ppm 59.8, 54.8, 32.0, 29.8, 29.74, 29.71, 29.69, 29.4, 27.9, 27.0, 26.1, 24.6, 22.8, 14.2. **GC-MS** (EI): m/z 309 (M⁺, 1%), 99 (7), 98 (100), 96 (1), 85 (1), 84 (1), 70 (1), 69 (1), 57 (1), 56 (1), 55 (4).

1-Octadecylpiperidine

CAS registry No. [79403-35-3]. **¹H NMR** (400 MHz, CDCl₃): δ/ppm 2.38 (br-s, 4H), 2.31–2.25 (m, 2H), 1.65–1.55 (m, 4H), 1.54–1.47 (m, 4H), 1.47–1.18 (m, 30H), 0.88 (t, 3H, J = 6.8 Hz). **¹³C NMR** (100 MHz, CDCl₃): δ/ppm 59.7, 54.7, 32.0, 29.8, 29.74, 29.70, 29.67, 29.4, 27.9, 26.9, 26.0, 24.5, 22.8, 14.2. **GC-MS** (EI): m/z 337 (M⁺, 1%), 336 (1), 99 (7), 98 (100), 96 (1), 85 (2), 84 (2), 70 (1), 69 (1), 57 (2), 56 (1), 55 (4).
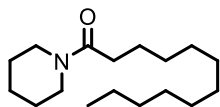
1-(1-Piperidinyl)-1-dodecanone (4)

CAS registry No. [22342-28-5]. **^{1}H NMR** (400 MHz, CDCl$_3$): δ/ppm 3.55 (t, 2H, J = 5.4 Hz), 3.39 (t, 2H, J = 5.4 Hz), 2.31 (t, 2H, J = 7.6 Hz), 1.69–1.48 (m, 8H), 1.38–1.19 (m, 16H), 0.88 (t, 3H, J = 7.0 Hz). **^{13}C NMR** (100 MHz, CDCl$_3$): δ/ppm 171.6, 46.8, 42.6, 33.6, 32.0, 29.7, 29.60, 29.57, 29.5, 29.4, 26.6, 25.7, 25.6, 24.7, 22.7, 14.2. **GC-MS** (EI): m/z 267 (M$^+$, 3%), 238 (1), 224 (1), 196 (1), 182 (2), 168 (1), 154 (4), 141 (5), 140 (23), 128 (8), 127 (100), 126 (3), 113 (2), 112 (21), 99 (3), 98 (1), 86 (7), 85 (14), 84 (21), 83 (2), 71 (1), 70 (7), 69 (12), 68 (1), 67 (1), 60 (2), 57 (9), 56 (7), 55 (10), 54 (1).

1-Dodecylpiperidine (3)

^{1}H NMR spectrum of 1-dodecylpiperidine
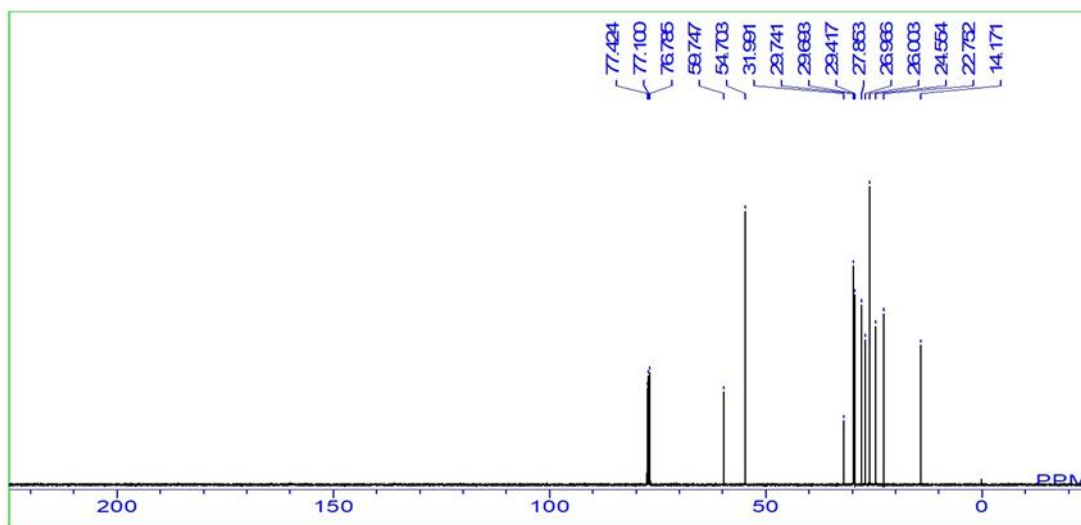
^{13}C NMR spectrum of 1-dodecylpiperidine
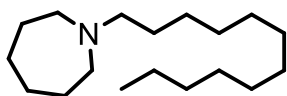
1-Dodecylazepane
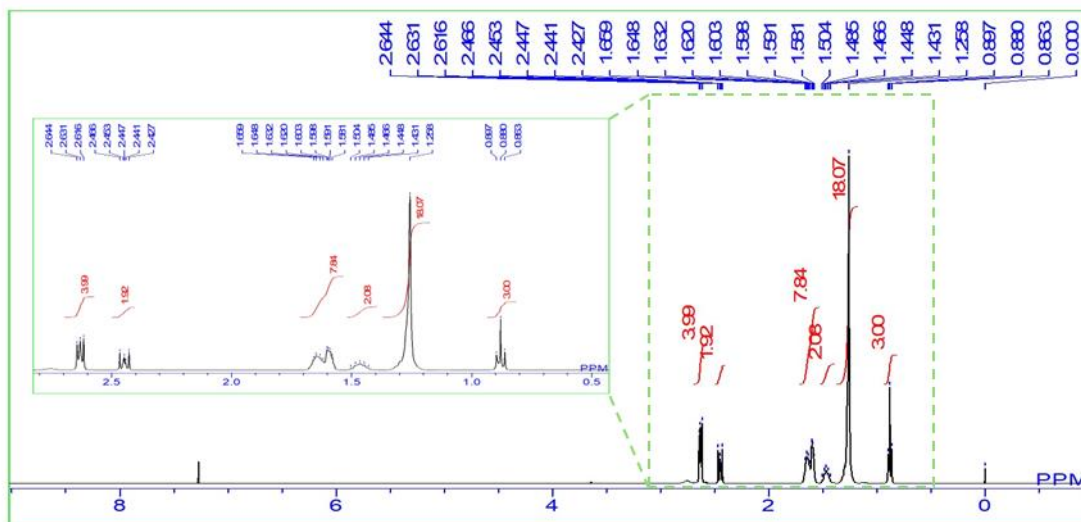
^{1}H NMR spectrum of 1-dodecylazepane
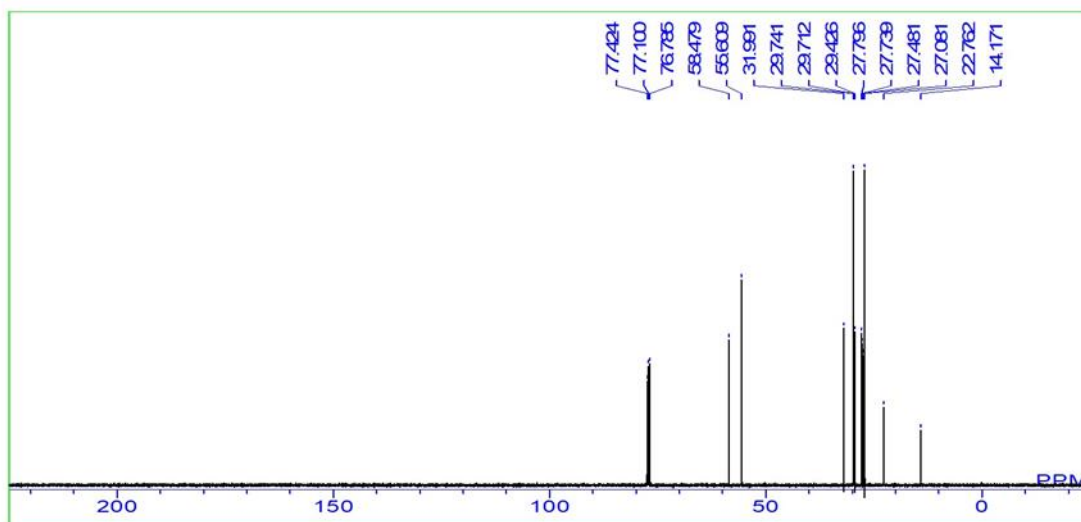
^{13}C NMR spectrum of 1-dodecylazepane
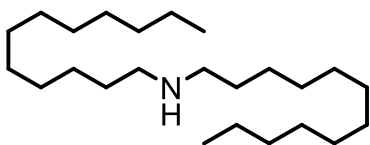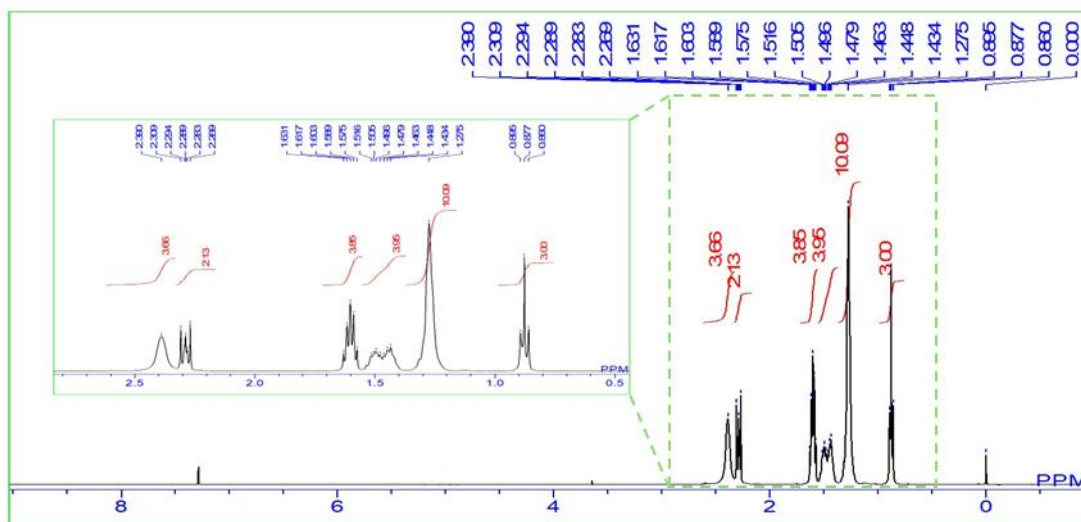
Didodecylamine
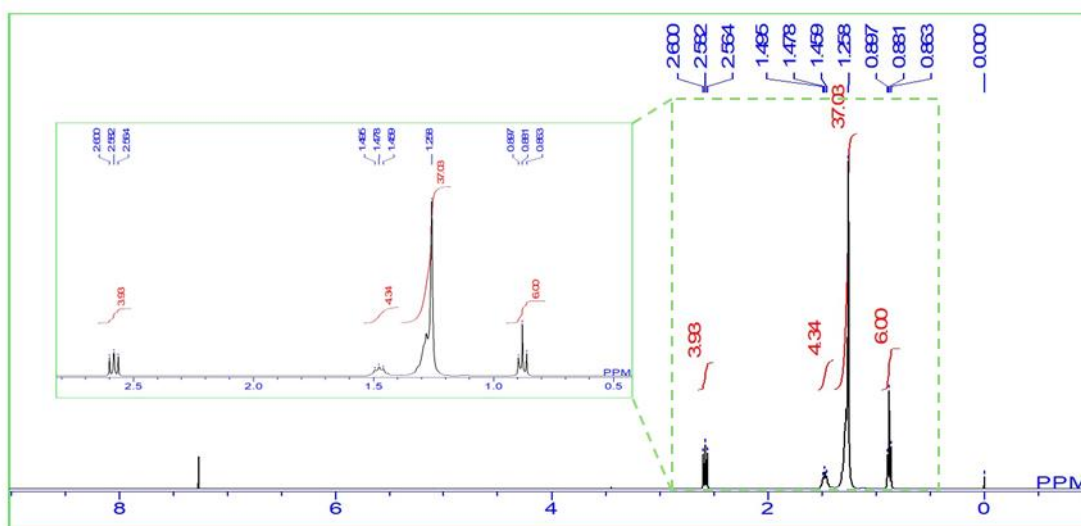
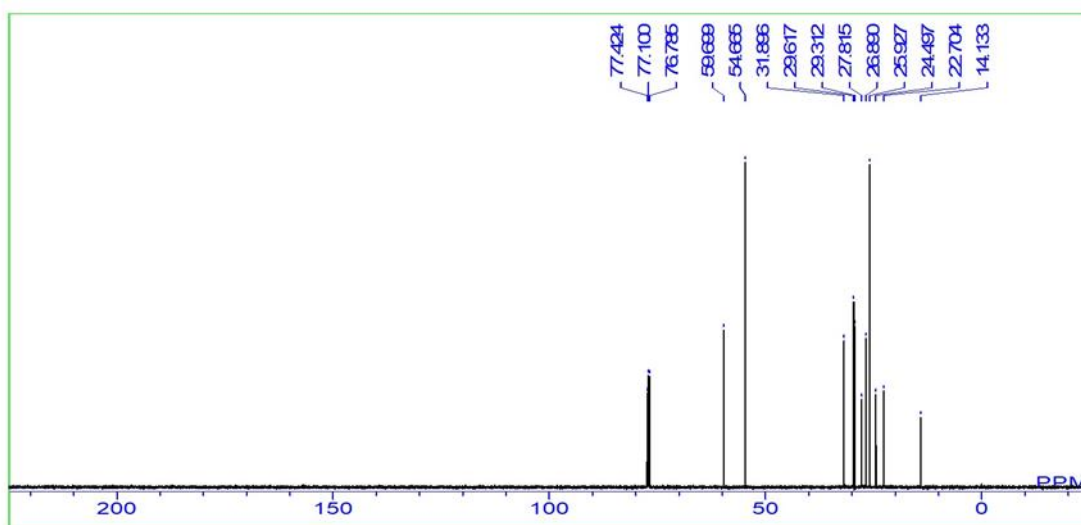
^{1}H NMR spectrum of didodecylamine
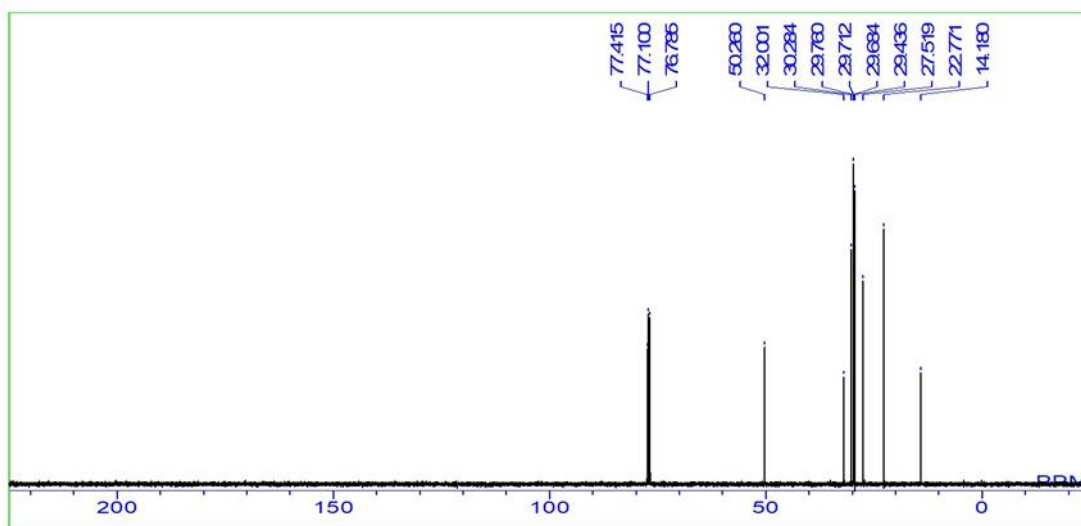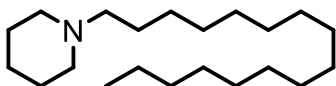

^{13}C NMR spectrum of didodecylamine
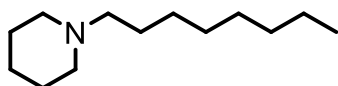
1-Octylpiperidine

^{1}H NMR spectrum of 1-octylpiperidine
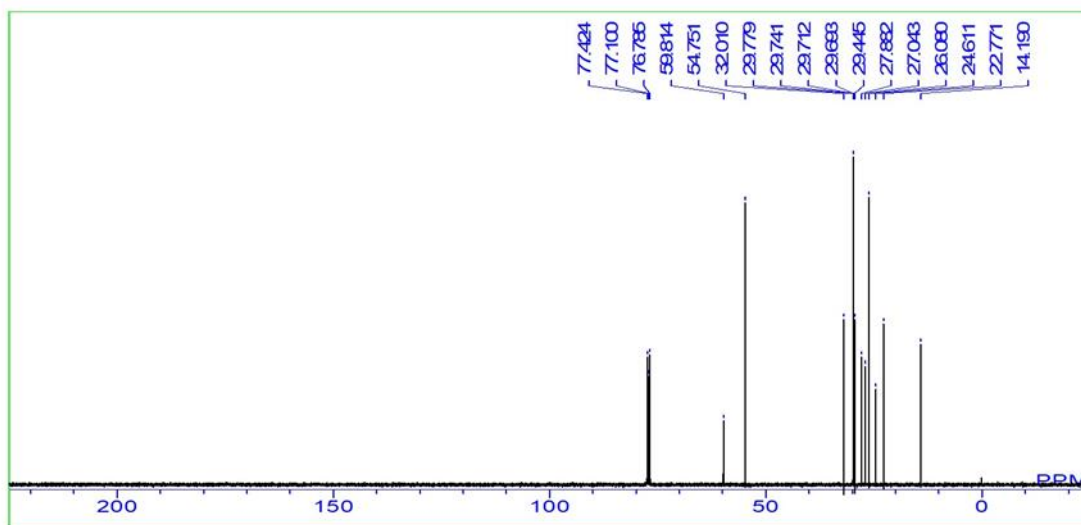

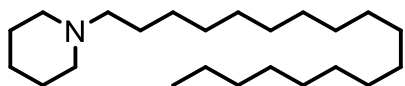^{13}C NMR spectrum of 1-octylpiperidine
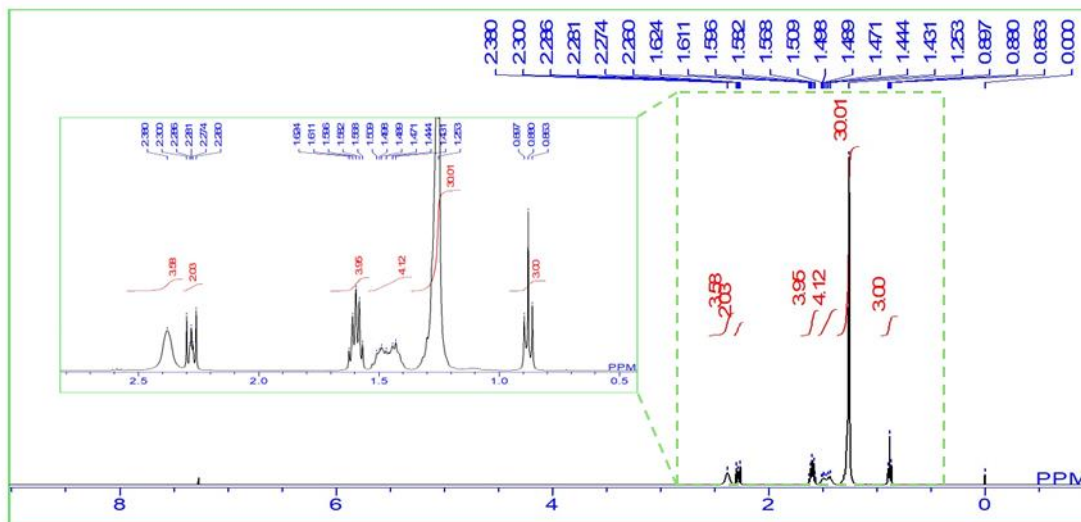
1-Hexadecylpiperidine
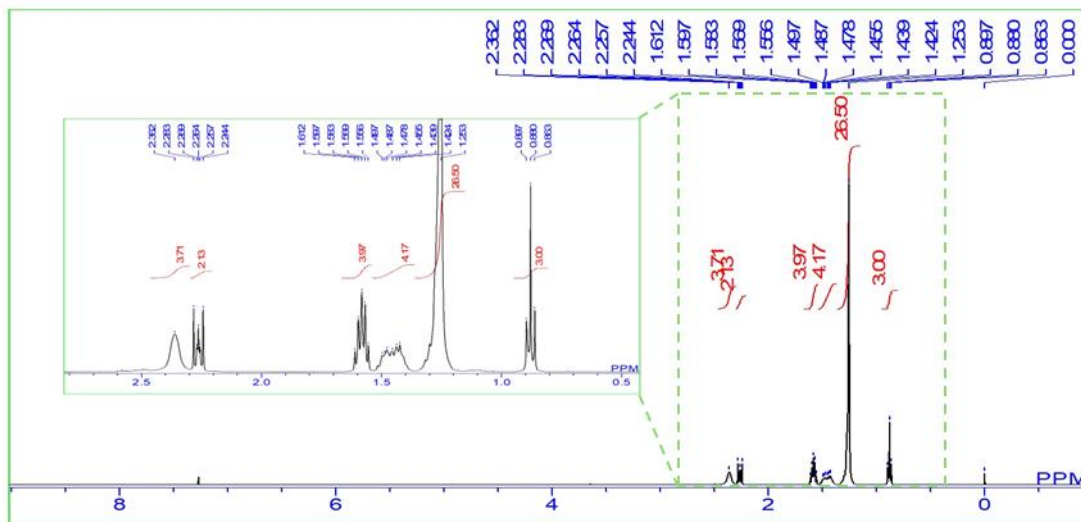
^{1}H NMR spectrum of 1-hexadecylpiperidine
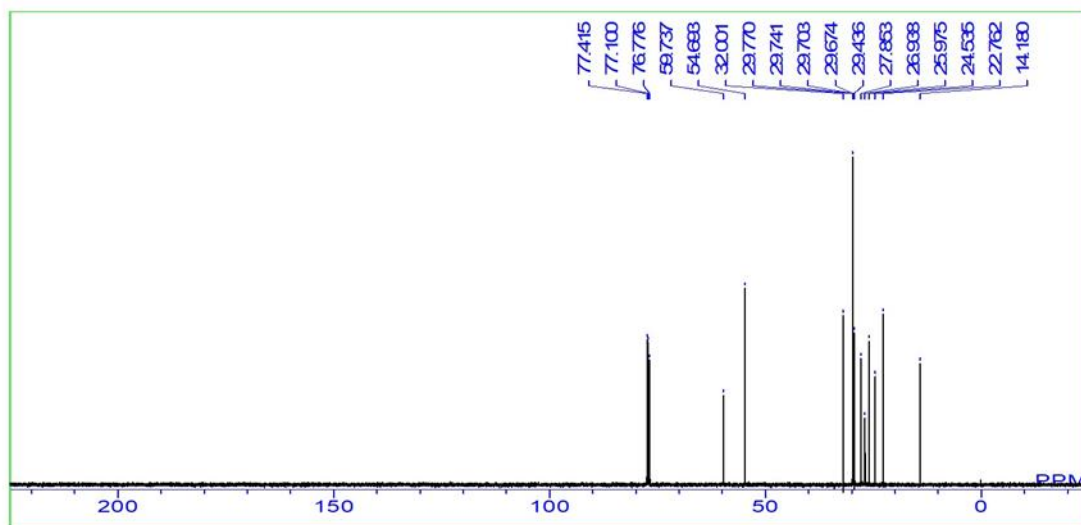

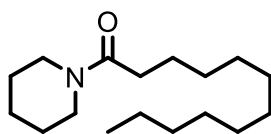^{13}C NMR spectrum of 1-hexadecylpiperidine
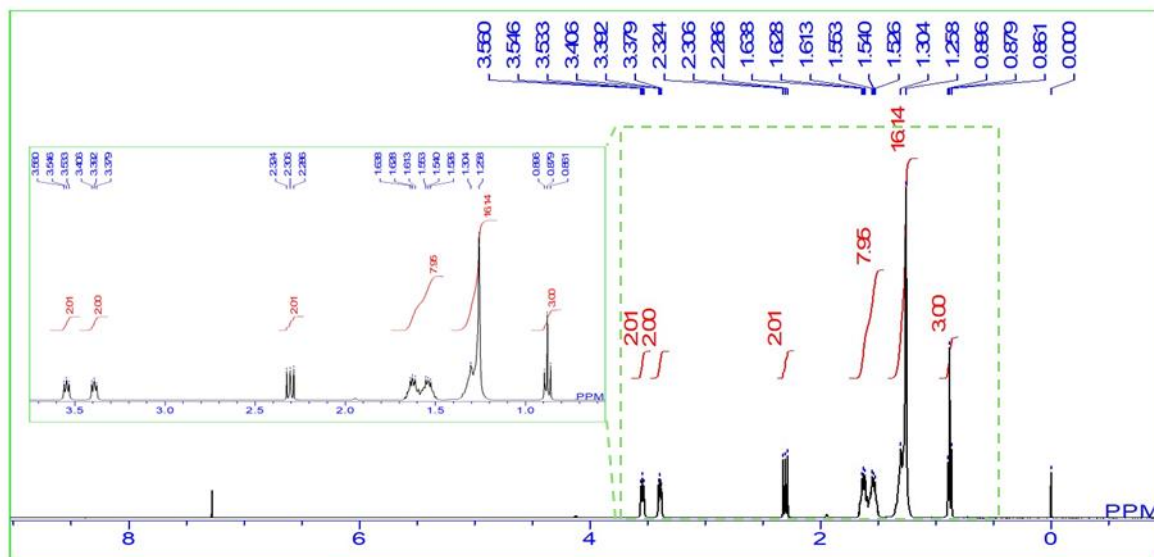
1-Octadecylpiperidine

^{1}H NMR spectrum of 1-octadecylpiperidine
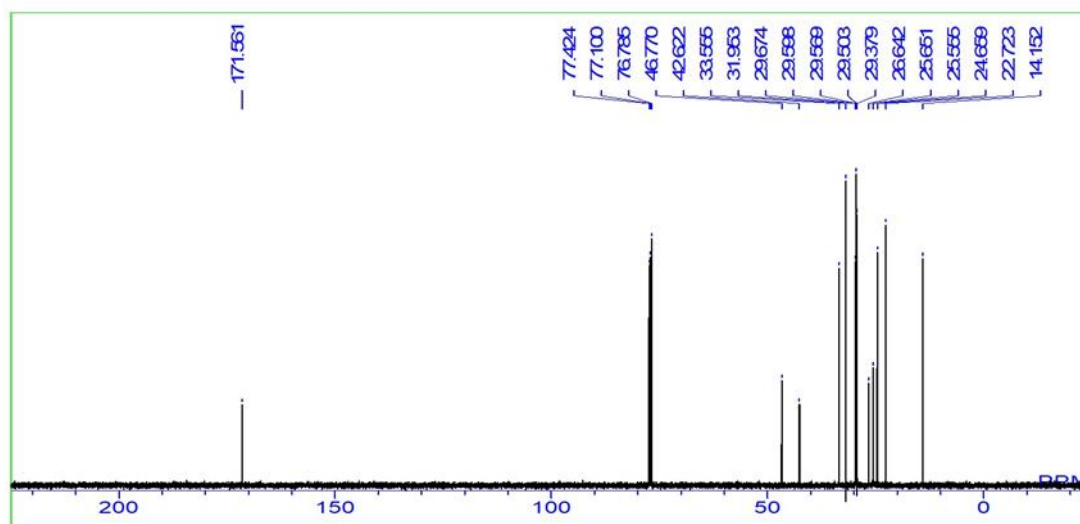

^{13}C NMR spectrum of 1-octadecylpiperidine

1-(1-Piperidinyl)-1-dodecanone (4)

^{1}H NMR spectrum of 1-(1-piperidinyl)-1-dodecanone

^{13}C NMR spectrum of 1-(1-piperidinyl)-1-dodecanone

7. References

S1. B. B. Michniak, M. R. Player, D. A. Godwin, C. C. Lockhart and J. W. Sowell, *Int. J. Pharm.*, 1998, **161**, 169–178.

S2. (a) F. Wei, G.-Z. Gao, X.-F. Wang, X.-Y. Dong, P.-P. Li, W. Hua, X. Wang, X.-M. Wu and H. Chen, *Ultrason. Sonochem.*, 2008, **15**, 938–942. (b) K. Yuan, Y. Yamazaki, X. Jin and K. Nozaki, *J. Am. Chem. Soc.*, 2023, **145**, 3454–3461.

S3. R. Adam, J. R. Cabrero-Antonino, K. Junge, R. Jackstell and M. Beller, *Angew. Chem. Int. Ed.*, 2016, **55**, 11049–11053.

S4. H. Rutzen, DE1288595B, 1969.

S5. M. A. R. Jamil, S. M. A. H. Siddiki, A. S. Touchy, M. N. Rashed, S. S. Poly, Y. Jing, K. W. Ting, T. Toyao, Z. Maeno and K. Shimizu, *ChemSusChem*, 2019, **12**, 3115–3125.

S6. A. I. Balabanovich, I. A. Klimovtsova, V. P. Prokopovich and N. R. Prokopchuk, *Thermochim. Acta*, 2007, **459**, 1–8.